Simultaneous Diagnosis and Gene Therapy of Immuno-Rejection in Rat Allogeneic Heart Transplantation Model Using a T-Cell-Targeted Theranostic Nanosystem

Yu Guo,[†,‡,⊥,∥] Wenjie Chen,[†,∥] Weiwei Wang,[‡,§,∥] Jun Shen,[⊥,*] Ruomi Guo,[⊥] Faming Gong,[§] Shudong Lin,[§] Du Cheng,[§] Guihua Chen,[†,*] and Xintao Shuai[‡,§,*]

[†]Lab of Liver Disease Hospital, Medical Research Center, Third Affiliated Hospital, Sun Yat-Sen University, Guangzhou 510630, China, [‡]Center of Biomedical Engineering, Zhongshan School of Medicine, Sun Yat-Sen University, Guangzhou 510080, China, [§]PCFM Lab of Ministry of Education, School of Chemistry and Chemical Engineering, Sun Yat-Sen University, Guangzhou 510275, China, and [⊥]Department of Radiology, Sun Yat-Sen Memorial Hospital, Sun Yat-Sen University, Guangzhou 510120, China

ABSTRACT As the final life-saving treatment option for patients with terminal organ failure, organ transplantation is far from an ideal solution. The concomitant allograft rejection, which is hardly detectable especially in the early acute rejection (AR) period characterized by an intense cellular and humoral attack on donor tissue, greatly affects the graft survival and results in rapid graft loss. Based on a magnetic resonance imaging (MRI)-visible and T-cell-targeted multifunctional polymeric nanocarrier developed in our lab, effective co-delivery of pDNA and superparamagnetic iron oxide nanoparticles into primary T cells expressing CD3 molecular biomarker was confirmed *in vitro*. In the heart transplanted rat model, this multifunctional nanocarrier showed not only a high efficiency in detecting post-transplantation acute rejection but also a great ability to mediate gene transfection in T cells. Upon intravenous injection of this MRI-visible polyplex of nanocarrier and pDNA, T-cell gathering was detected at the endocardium of the transplanted heart as linear strongly hypointense areas on the MRI T_2*-weighted images on the third day after cardiac transplantation. Systematic histological and molecular biology studies demonstrated that the immune response in heart transplanted rats was significantly suppressed upon gene therapy using the polyplex bearing the DGKα gene. More excitingly, the therapeutic efficacy was readily monitored by noninvasive MRI during the treatment process. Our results revealed the great potential of the multifunctional nanocarrier as a highly effective imaging tool for real-time and noninvasive monitoring and a powerful nanomedicine platform for gene therapy of AR with high efficiency.

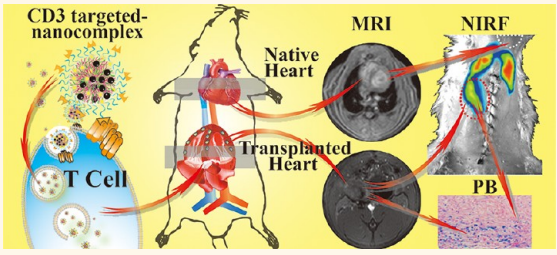

KEYWORDS: nanoparticle · single-chain antibody · T-cell targeting · magnetic resonance imaging · heart allograft rejection

Organ transplantation has achieved great success in patients with terminal organ failure resulting from a variety of diseases; however, the biggest challenge in this life-saving treatment is still the concomitant allograft rejection resulting from severe immune response,[1−3] which needs not only a highly effective diagnosis especially in the early acute rejection (AR) period but also a proper treatment.[4−8] It was known that cells of the adaptive immune system, in particular, T cells, play a central role in the AR of most allografts.[9,10] The process of AR was initiated once the host T cells gathered in grafts and conducted allo-recognition.[1,11] Therefore, T-cell-based early diagnosis and immuno-suppressive therapy are of extreme importance for achieving better graft survival.

Modern imaging techniques such as computed tomography (CT), magnetic resonance imaging (MRI), and positron emission tomography (PET) have demonstrated great success in the diagnosis of various fatal diseases. Unfortunately, very few reliable imaging tools have been developed thus far for the early detection of AR,[4−8] in which highly specific imaging probes for T cells are required. As for the post-transplantation therapy of AR, small molecular immuno-suppressive drugs such as Tacrolimus (FK506) have demonstrated high

* Address correspondence to shenjun@mail.sysu.edu.cn, chgh1955@263.net, shuaixt@mail.sysu.edu.cn.

Received for review August 17, 2012 and accepted November 28, 2012.

Published online November 28, 2012
10.1021/nn3037573

efficiency in suppressing T-cell activity for immunosuppression treatment of allograft AR and in prolonging graft survival time.[12] The shortcomings of using these drugs are undesirable therapeutic index and considerable toxicity.[3,4] Moreover, lifelong immunosuppressive medication may result in patient susceptibility to infections, tumorigenesis, and other side effects.[4,5] The gene therapy had been shown to be able to achieve immuno-suppression of T cells with better durability, less toxicity, and cost-effectiveness.[6] However, a major problem of the promising gene therapy is that T cells are refractory to most of the current viral and nonviral gene delivery techniques.[1,2,7−10] The above situation has highlighted the urgent clinical need for new strategies that can diagnose and suppress AR more effectively.[1−3]

Recent advances in the emerging polymeric nanomedicine, especially success in the ligand-enabled active targeting of various cell types and the combination of imaging function with drug or gene therapy, that is, the so-called "theranostic" strategy, have made it possible to simultaneously monitor T-cell gathering and achieve effective immuno-modulation of T cells *via* gene therapy.[10,11,13−15] Our group recently developed a MRI-visible and CD3 single-chain antibody (scAbCD3)-targeted multifunctional polymeric nanocarrier for gene delivery to T cells, in the hope of concurrently detecting and inhibiting AR. Preliminary *in vitro* investigations in HB8521 cells, a rat T lymphocyte line, showed that the gene transfection efficiency was increased to 82% from only 7% upon functionalizing the nanocarrier with scAbCD3.[16] It has been reported that the diacylglycerol kinase (DGK) phosphorylates diacylglycerol to produce phosphatidic acid, leading to decreased and increased levels of these two lipid messengers that play a central role in T-cell activation. Overexpression of DGKα could result in a defect in T-cell receptor signaling that is characteristic of anergy. When stimulated in anergy-producing conditions, T cells lacking DGKα or DGK-f proliferated and produced interleukin-2 (IL-2).[17,18] Delivery of the therapeutic gene DGKα into rat T cells resulted in a 43% inhibition of cell proliferation and a 38% down-regulation of IL-2 expression, which indicated effective cell anergy due to the nanocarrier-mediated gene therapy. Moreover, the targeted gene delivery *in vitro* was trackable on the clinical MRI scanner.[16]

The exciting *in vitro* results have driven us to investigate whether this multifunctional nanocarrier system can mediate efficient gene transfection in primary T cells, as well, and whether it can provide simultaneous MRI probing and gene transfection in T cells during immuno-therapy of AR *in vivo* (Figure 1). Herein, we describe our results obtained in a heterotopic heart transplantation rat model as the first demonstration of a polymeric theranostic nanosystem with a combined feature of MRI function and targeted gene delivery for coincident diagnosis and treatment of post-transplantation AR *in vivo*.

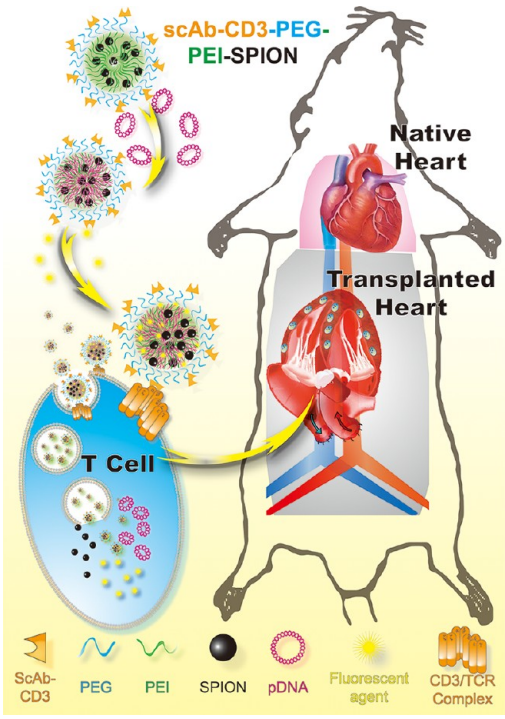

Figure 1. Schematic diagram of therapeutic process of magnetic targeting polyplex scAbCD3-PEG-g-PEI-SPION *in vitro* and *in vivo*.

RESULTS AND DISCUSSION

Synthesis and Gene Transfer of Theranostic Nanosystem. The nanocarrier (scAbCD3-PEG-g-PEI-SPION), which was the complex of poly(ethylene glycol)-grafted polyethylenimine (PEG-g-PEI), was functionalized with the CD3 single-chain antibody (scAbCD3) and superparamagnetic iron oxide nanoparticles (SPION), as shown in Figure 1. Polyplex of the multifunctional nanocarrier and pDNA formed at a nitrogen/phosphorus (N/P) ratio of 10, which was termed "theranostic nanosystem", was used in the present study because this formulation showed excellent pDNA condensation, high gene transfection efficiency, and low cytotoxicity in the rat HB8521 T lymphocyte line, as described in the previous work.[16] The MRI relaxivities and morphology of the polyplex used are shown in Figure 2. The measured particle size and zeta-potential of polyplex in PBS were, respectively, 106 nm and +19 mV.[16] The size of the polyplex in the rat serum appeared to have no significant change over 96 h, as shown in Figure S1 in Supporting Information. The polyplex demonstrated fairly low cytotoxicity in primary T cells, as well (Figure 2).

To show the cellular uptake and intracellular distribution of the polyplex, multiple fluorescent labelings of pDNA-DGKα and the vector were conducted. After 1 h incubation, the intracellular distribution pattern

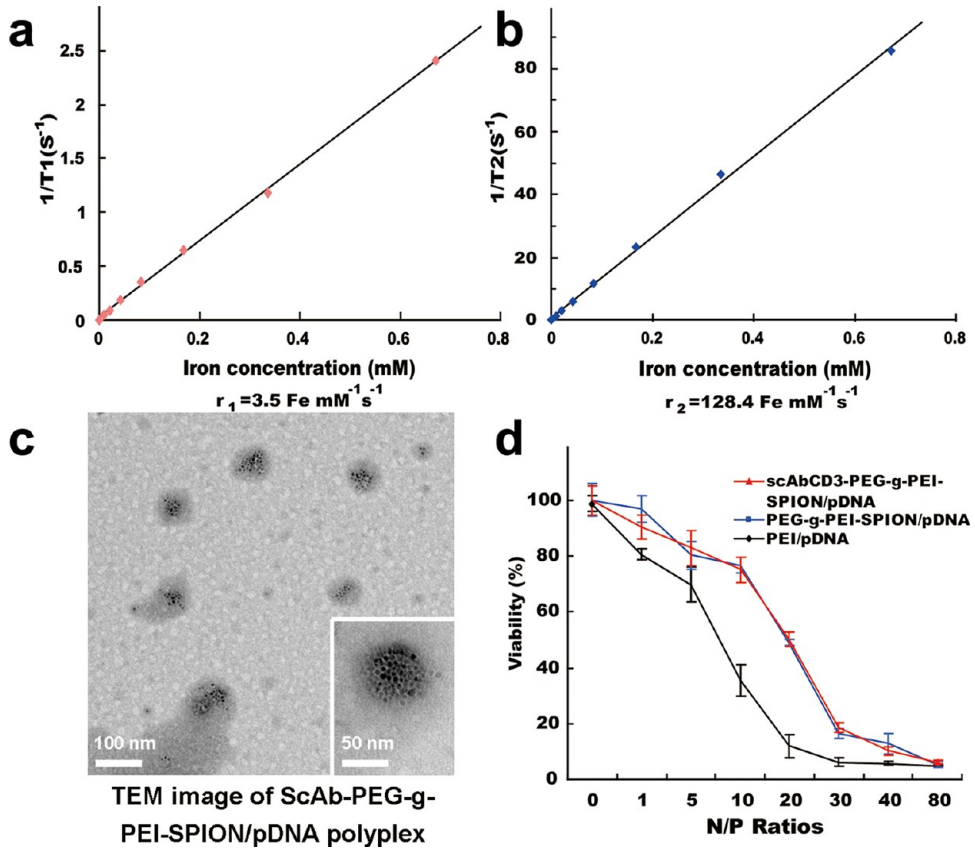

Figure 2. Characteristics of the polyplex. (a) Magnetic resonance T_1 relaxivities of the polyplex. (b) Magnetic resonance T_2 relaxivities of the polyplex. (c) Size and morphology of the polyplex analyzed using transmission electron microscopy. The dark and gray halo around the SPION cluster incorporated in the polyplex indicates a polymeric shell. The inset shows the magnified view of a single polyplex nanoparticle with the SPION cluster embedded inside the polymeric shell. (d) *In vitro* cytotoxicity assay. Cytotoxicity of the polyplexes at various nitrogen/phosphorus (N/P) ratios in rat primary T cells determined using CCK8 assay (pDNA amount: 0.15 mg per well, $n = 4$).

of scAbCD3-PEG-g-PEI-SPION (green fluorescence) is identical to that of pDNA-DGKα (red fluorescence) in the observation of cells using confocal laser scanning microscopy (CLSM) (Figure 3a and Figure S2 in Supporting Information), suggesting that pDNA-DGKα was delivered into the primary T cells by the CD3 targeted delivery agent. In addition, images of single fluorescence show that the cell membrane had more intensive red and green fluorescence than the cytoplasm, implying that a great number of polyplex nanoparticles were still in the process of crossing the cell membrane when cells were incubated for 1 h.

In line with the results obtained in the T lymphocyte line, functionalization of polyplex with scAbCD3 remarkably enhanced its cellular uptake by primary T cells, as well, leading to a much increased transfection efficiency of the delivered pDNA encoding for the reporter gene, enhanced green fluorescent protein (EGFP), which fluoresces much more intensely than wild-type GFP and is readily detectable using techniques of macroscopic imaging, fluorescence microscopy, or flow cytometry.[19] The scAbCD3-targeted polyplex showed a significantly higher gene transfection efficiency than the nontargeted counterpart (the percentage of EGFP-positive cells: 60.8 ± 2.48% *vs* 1.07 ± 0.21%, $P < 0.05$), as shown in Figure 3b. The expression of the therapeutic DGKα gene was then examined at mRNA and protein levels using the reverse transcription PCR and Western blotting assays, respectively. Compared to cells transfected with the nontargeted polyplex or PBS, cells transfected with the targeted polyplex showed obviously higher mRNA level and a stronger protein band of the DGKα gene (Figure 3c). These results demonstrated that scAbCD3-PEG-g-PEI-SPION could mediate highly effective gene transfection in primary T cells similarly as previously verified in T lymphocyte lines.

Early Detection of Acute Rejection (AR) by *In Vivo* Imaging. The MRI-visible theranostic nanosystem enables simultaneous MRI and optical imaging of its *in vivo* T-cell-targeted delivery. We first monitored the localized T-cell gathering in heart transplanted rats using noninvasive MRI at designed post-transplantation time points. Then optical imaging was obtained with near-infrared fluorescence (NIRF) imaging by using the Alexa Fluor 680 as the reporter. All animals receiving injection of the MRI-visible polyplexes showed a darkening effect in the spleen and liver, which is

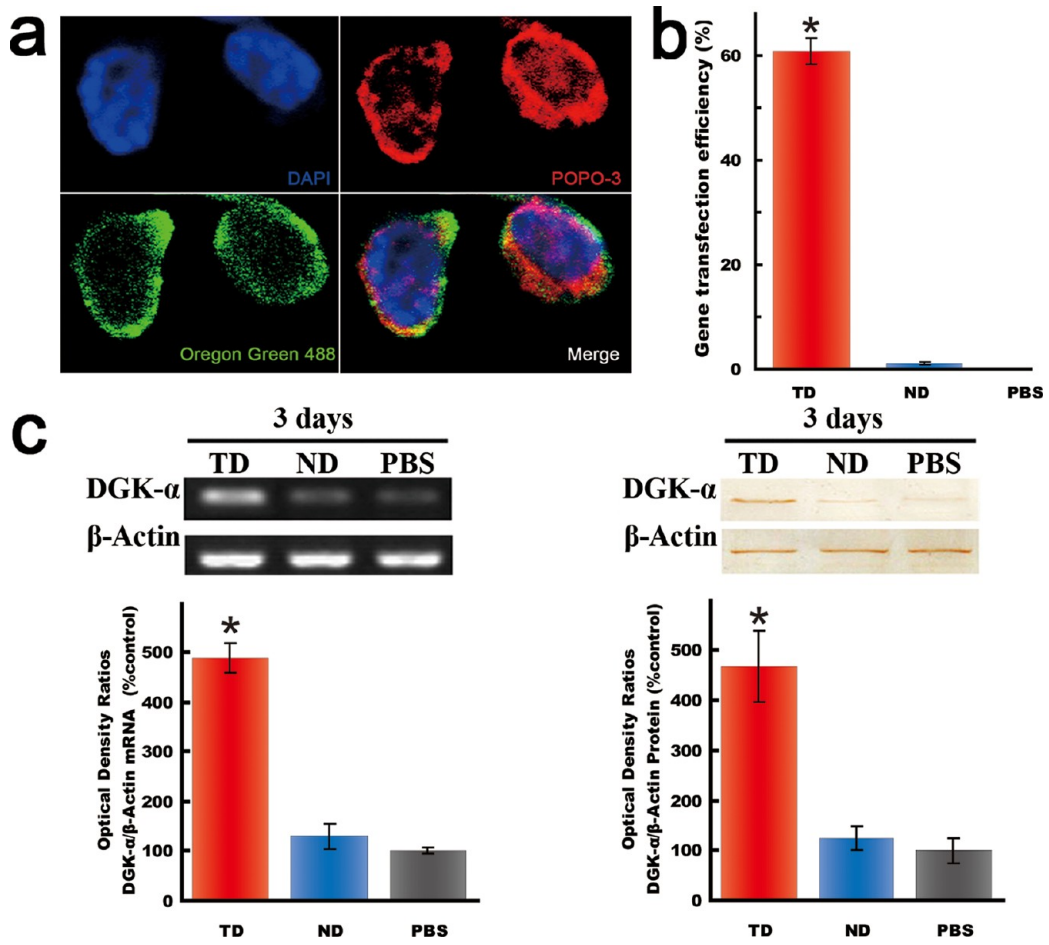

Figure 3. Gene transfection in primary T cells. (a) Laser confocal microscope images (magnification: 1000×) of primary T cells after 1 h incubation with scAbCD3-PEG-g-PEI-SPION/pDNA-DGKα in RPMI 1640 medium. Blue, DAPI for nucleus; red, POPO-3 for pDNA plasmid; green, Oregon Green 488 for delivery agent. (b) Relative transfection efficiency of the reporter gene, enhanced green fluorescence protein (EGFP) in primary T cells as determined by flow cytometry 3 days after transfection ($n = 3$, $^*P < 0.05$, compared with PBS group). (c) mRNA level (left) and protein expression level (right) of DGKα in primary T cells 3 days after incubation with the targeted polyplex (TD, scAbCD3-PEG-g-PEI-SPION/pDNA-DGKα), nontargeted polyplex (ND, PEG-g-PEI-SPION/pDNA-DGKα), and PBS, as determined by RT-PCR and WB, respectively ($n = 3$, $^*P < 0.05$, compared with PBS group) .

consistent with the fact that nanoparticles are prone to nonspecific deposition in the reticuloendothelial sites. The rats receiving targeted polyplex-containing null plasmid (scAbCD3-PEG-g-PEI-SPION/pDNA, the TN group) showed strongly hypointense areas on the MRI-balanced turbo field echo (bTFE) images of the transplanted heart during the post-transplantation period from 0 to 10 days (Figure 4a,c), implying accumulation of the targeted polyplex in the allograft. bTFE belongs to a steady-state free precession pulse sequence producing images with a high temporal resolution and increased signal from fluid along with retaining T_1-weighted tissue contrast that are particularly useful in cardiac MRI.[20] In particular, the endocardium of the transplanted heart showed a dark linear signal on the T_2*-weighed images acquired on the third and tenth days post-transplantation. On the contrary, the MRI signal intensity of the native heart (NH) of the rats remained unchanged throughout the experiment, indicating that the targeted polyplex did not accumulate in the native heart. This result is conceivable because T cells did not accumulate in the native heart absent of an immune rejection. Furthermore, the rats receiving the nontargeted polyplex-containing null plasmid (PEG-g-PEI-SPION/pDNA, the NN group) showed little change as well in the MRI signal intensity of the transplanted heart.

This result indicates that, although T cells had accumulated in the allograft as detected by the targeted polyplex, such event was not detectable by the nontargeted polyplex lacking specific binding ability to T cells. Taken together, these results evidenced the high efficiency of the scAbCD3-targeted theranostic nanosystem in probing the localized T-cell accumulation *in vivo*, which reflects the AR level after organ transplantation. More excitingly, no obvious hypointense signal or decline of MRI signal intensity was detected in the allograft of rats receiving treatment using polyplex containing the therapeutic DGKα plasmid (scAbCD3-PEG-g-PEI-SPION/pDNA-DGKα, the TD

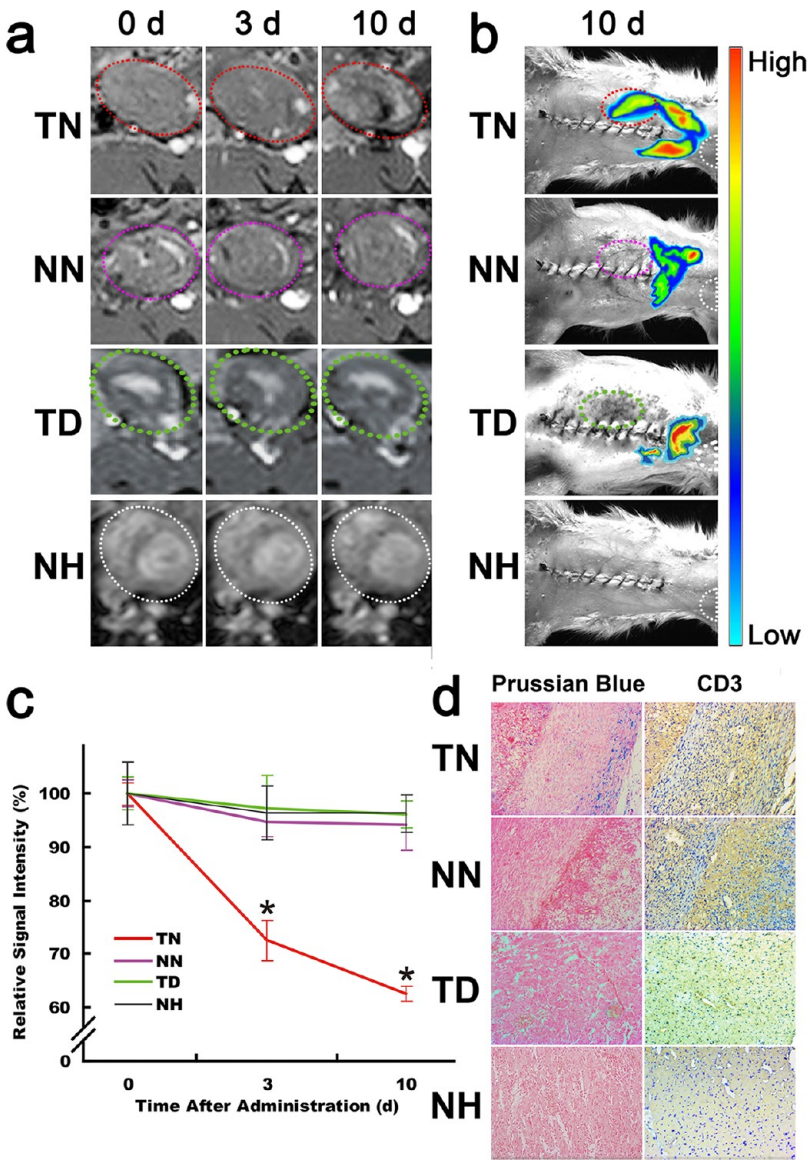

Figure 4. Early detection of acute rejection by noninvasive, *in vivo* imaging in rat allogeneic heart transplantation model after treatment with null plasmid-containing polyplex. (a) Magnetic resonance images (MRI) of transplantation model during the period from 0 to 10 days after transplantation. Areas marked with dashed red, purple, and green circles illustrate the grafted hearts in the animals treated with scAbCD3-PEG-g-PEI-SPION/pDNA(TN), PEG-g-PEI-SPION/pDNA (NN), and scAbCD3-PEG-g-PEI-SPION/pDNA-DGKα(TD), respectively. White circles show the native hearts (NH). (b) Near-infrared fluorescence (NIRF) imaging of transplantation model during the period on the tenth day after transplantation. The dashed red, purple, green, and white circles show the same areas as in panel a. The fluorescent reporter used for NIRF is Alexa Fluor 680. (c) MRI signal intensity change of the transplanted heart during the period from 0 to 10 days after transplantation (n = 12, $^*P < 0.05$, compared with NH). (d) Prussian blue staining and histologic CD3 antibody analysis of the graft tissues from the TN, NN, TD groups, and NH (magnification: 100×), on the third day after transplantation. The positive Prussian blue staining is shown by blue color, and the positive CD3 immuno-histochemistry staining is shown by brown color.

group) at all post-injection time points (Figure 4a,c and Figure S3a,c in Supporting Information), which strongly demonstrated that the therapeutic DGKα gene delivered by the T-cell-targeted theranostic nanosystem has effectively suppressed the acute immune rejection in the allograft and thus led to a significantly decreased level of T-cell accumulation there.

Near-infrared fluorescence (NIRF) imaging was performed to verify the results of the MRI by using Alexa Fluor 680 labeling of the MRI-visible theranostic nanosystem. As shown in Figure 4b and Figure S3b in Supporting Information, strong NIRF signal was obtained in the graft area of the TN group, whereas almost no NIRF signal was detected in both the native heart and graft in the other two experimental groups (the NN and TD groups). These results once again confirmed that T-cell gathering happened in the graft, but this event could be probed only by the scAbCD3-targeted polyplex. In addition, the polyplexes showed spleen accumulation, as shown by MRI experiments, as well (Figure S4 in Supporting Information).

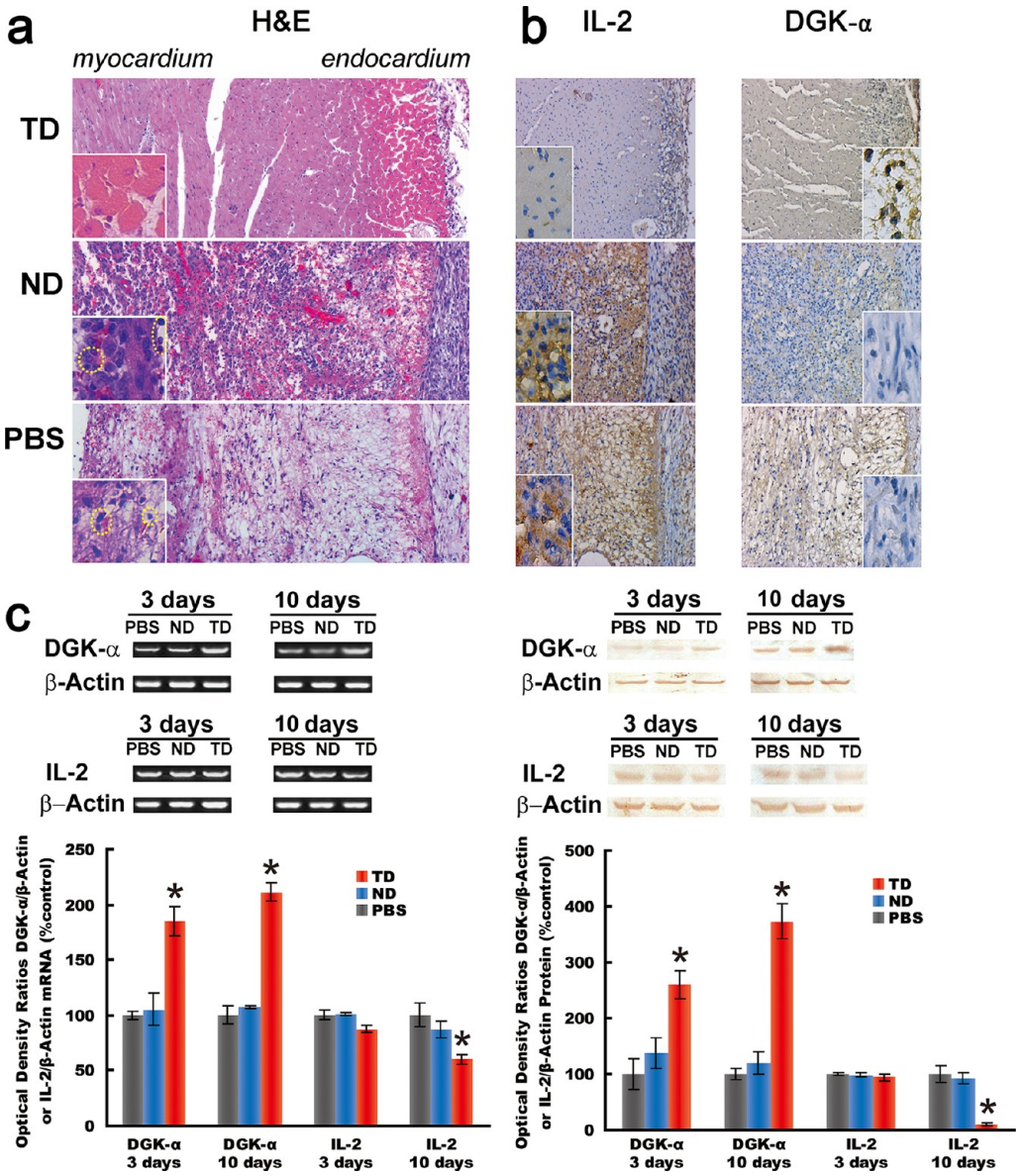

Figure 5. Histological and immuno-chemical results. (a) H&E staining of the graft tissues from the TD (scAbCD3-PEG-g-PEI-SPION/pDNA-DGKα), ND (PEG-g-PEI-SPION/pDNA-DGKα), and PBS groups on the 10th day after transplantation (magnification: 100×; inset magnification: 400×). The IL-2 immuno-histochemistry staining (brown) is present in extracellular space and cytoplasm. The DGKα immuno-histochemistry staining (brown) is present in cytoplasm. Areas marked with dashed yellow circles show the T cells gathering in the graft tissues. (b) IL-2 and DGKα immuno-histochemical analyses of the graft tissues from the TD, ND, and PBS groups on the 10th day after transplantation (magnification: 100×; inset magnification: 400×). (c) mRNA level (left) and protein expression level (right) of DGKα and IL-2 determined by RT-PCR or Western blotting in T cells from the peripheral blood of the TD, ND, and PBS groups on the third and tenth days after transplantation (n = 12; *P < 0.05, compared with PBS group).

Further immuno-histochemical staining for CD3 antigen and Prussian blue staining for iron are highly supportive of the above results observed in MRI and NIRF imaging experiments. Without the DGKα gene therapy, CD3 antigen of T cells was verified to be present in transplanted heart but was absent in the native one, and Prussian blue staining of the graft tissues from the TD group demonstrated that most of the infiltrated T lymphocytes were transfected by the theranostic nanosystem (Figure 4d). In particular, strong blue iron stains were observed in T cells infiltrated into the endocardium of the allograft.

Histological and Immunohistochemical Studies. The multifunctional capacity of the T-cell-targeted theranostic nanosystem as a sensitive MRI probe for resultant T-cell gathering from immuno-rejection and as an effective vector to mediate T-cell-targeted gene therapy for prevention of acute rejection (AR) was further investigated using histological and immuno-histochemical analyses on the tenth day after transplantation (Figure 5a,b).

In the histological analysis, the tissues of cardiac grafts from the tissues of animals treated with the PBS (the PBS group) or PEG-g-PEI-SPION/pDNA-DGKα (the ND group) exhibited signs of IV and IIIB grades of

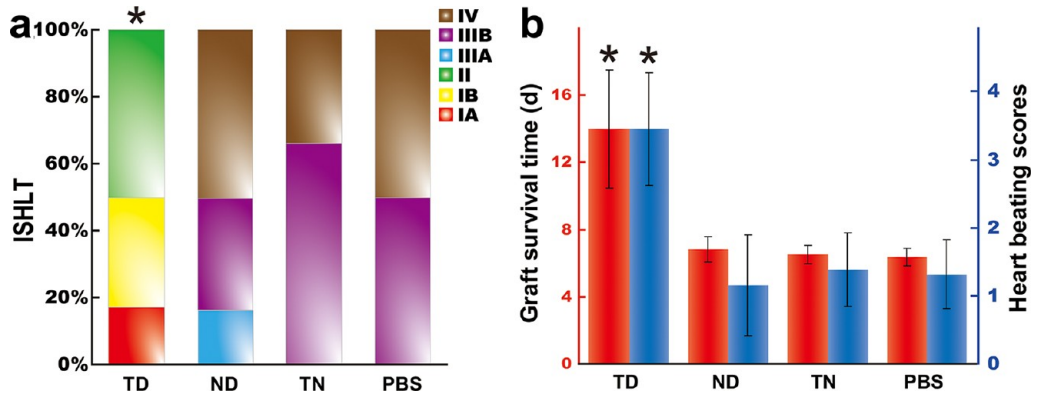

Figure 6. General situation of transplanted hearts. (a) AR grades of the TD (scAbCD3-PEG-g-PEI-SPION/pDNA-DGKα), ND (PEG-g-PEI-SPION/pDNA-DGKα), TN (scAbCD3-PEG-g-PEI-SPION/pDNA), and PBS groups assessed according to the grading system of the International Society for Heart and Lung Transplantation (ISHLT) (n = 12, *P < 0.05, compared with PBS group). (b) Graft survival time and 6 days post-operation heart beating score (HBS) of the transplanted allografts (n = 12; *P < 0.05, compared with PBS group).

immuno-rejection, which were featured as massive lymphocyte infiltration in both myocardium and endocardium, coagulative myocyte necrosis, scattered hemorrhage, and severe vasculopathy (Figure 5a and Figure 6a). In contrast, H&E staining of graft tissue sections from the targeted therapeutic group (the TD group) showed much weaker immuno-rejection, which fit into I and II grades of AR (Figure 5a and Figure 6a), where vasculopathy only occurred in much more circumscribed areas of cardiac allograft; no myocardium necrosis was detected, and lymphocyte infiltration mostly was observed in endocardial membranes but with significantly reduced number, as compared to that of the ND and PBS groups.

In the immuno-histochemical analysis (Figure 5b,c), the graft tissues from animals of the PBS and ND groups showed dispersive IL-2 expression in the massive infiltrated T lymphocytes and their surrounding myocardium or endocardium. Comparatively, myocardium of the graft tissues from the TD group showed almost nonappreciable IL-2 expression, and only subtle IL-2 expression was detected in the endocardial membranes where a much punctuated DGKα expression occurred in infiltrated T lymphocytes there. It was noteworthy that a much lower level of IL-2 expression was also found as determined by ELISA assay of the serum of animals from the TD group (Figure S5 in Supporting Information). Moreover, more significant DGKα expression whereas less IL-2 expression was detected by reverse transcription PCR and Western blotting analyses in the T cells from the peripheral blood of the TD group (Figure 5c), and these cells showed less proliferation in response to stimulation of ionomycin and PMA than that of the ND and PBS groups, as determined by [^{3}H] thymidine assay (Figure S6 in Supporting Information).

The above results strongly demonstrate that the CD3-targeted theranostic nanosystem administered by intravenous injection was able to identify the T lymphocytes *in vivo* and induce their anergy *via* gene therapy, which is regarded as the underlying reason for depressed immuno-rejection in rats receiving allogeneic heart transplantation.

Therapeutic Effect of Theranostic Nanosystem Containing DGKα. After heterotopic heart transplantation, the transplanted rats did not exhibit notable signs of diarrhea, discomfort, or neurologic dysfunction throughout the experiment. The grafts were monitored by daily abdominal palpation to assess the heart beating score (HBS). For most animals of the ND and PBS groups, HBS reached 0 on the seventh day post-transplantation. As shown in Figure 6b, on the sixth day post-transplantation, the HBS of the TD group was obviously higher than that of the ND and PBS groups (3.5 ± 0.8 *vs* 1.17 ± 0.76 and 1.33 ± 0.52, respectively, P < 0.05). Furthermore, the graft survival time of the TD group was significantly longer than that of the ND and PBS groups (Figure 6b, 14 ± 3.5 days *vs* 6.8 ± 0.75 days and 6.3 ± 0.52 days, respectively, P < 0.05). These results demonstrate the excellent outcome of the immuno-suppressive effect of the DGKα gene on the account of the CD3-targeted theranostic nanosystem. In contrast, injection of the nontargeted theranostic nanosystem bearing the DGKα gene (*i.e.*, the ND group) had no obvious therapeutic benefit in immuno-suppression, which highlights again the significance of the CD3-antibody-mediated T-lymphocyte-specific gene delivery *in vivo*.

Techniques which have a capacity for simultaneous detection and effective treatment of AR after allograft transplantation are not available yet. The current study aimed at exploring the potential of combining diagnosis and gene therapy of T-cell-based acute immuno-rejection in allogeneic heart transplantation rat model using the CD3-targeted theranostic nanosystem, which was recently developed in our lab.

It is well-known that diagnosis and therapy of allograft rejection is a lifelong challenge for patients who had undergone organ transplantation.

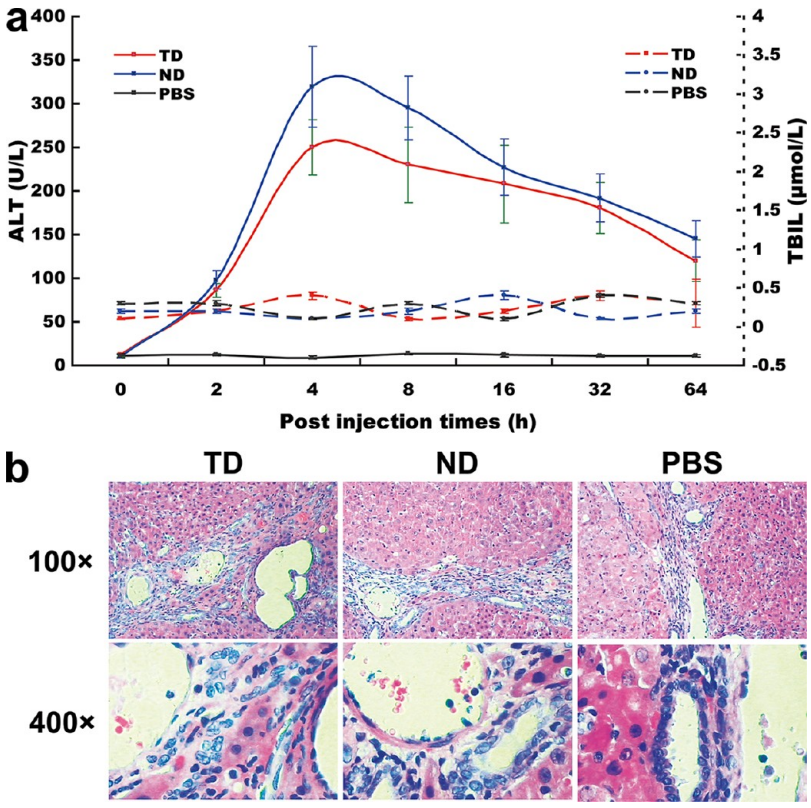

Figure 7. *In vivo* **toxicological studies. (a) Serum alanine transaminase (ALT) levels and total bilirubin (TBIL) were assessed after injection of the polyplexes. The serum ALT levels increased from 2 to 4 h after injection, afterward, gradually declined in TD (scAbCD3-PEG-g-PEI-SPION/pDNA-DGKα) and ND (PEG-g-PEI-SPION/pDNA-DGKα) groups, while no obvious change in TBIL levels appeared in TD, ND, and PBS groups. (b) H&E staining of the hepatic tissues from TD, ND, and PBS groups on the tenth day after injection showed no bleeding and no obvious hepatocellular or biliary necrosis.**

Current immuno-suppressive therapy mainly uses small molecular drugs, which encounters a lot of problems resulting from the short half-lives and insufficient cell specificity of the drugs. Therefore, new therapeutic approaches that may overcome the shortages of small molecular drugs are in an urgent clinical need nowadays. In the present study, immunosuppression was attempted using gene therapy mediated by a multifunctional MRI-visible nanocarrier that can specifically bind to the CD3 antigen, a coreceptor complex of the T-cell receptor. The results show that the CD3-targeted theranostic nanosystem may effectively transport the DGKα gene into primary T lymphocytes, resulting in a high gene transfection efficiency, while the nontargeted theranostic nanosystem lacks such effect. Molecular biology studies confirmed high expression level of the DGKα gene in the endocardium of the transplanted heart and, consequently, significantly suppressed expression of IL-2 in cardiac graft tissues and peripheral blood, as well. IL-2 is a major functional cytokine of T cells secreted by activated T cells and plays a key role in T-cell proliferation in response to stimulation. It is considered as a symbol of rejection that is monitored after organ transplantation.[21−23] Therefore, the suppressed expression of IL-2 implies that T-cell anergy has been effectively induced *in vivo* after treatment of the CD3-targeted theranostic nanosystem. It is noted that the treatment did not cause obvious side effects. These results suggested the great potential of the CD3-targeted theranostic nanosystem in mediating effective gene therapy for immuno-suppression after organ transplantation.

On the other hand, early detection and dynamic monitoring of immuno-rejection is crucial for planning effective immuno-suppressive therapy after organ transplantation. Currently, graft biopsy remains the gold standard for diagnosis of acute rejection. However, small sample biopsy is susceptible to sampling error, and even worse, it is invasive and thus associated with high risk.[4,5,24] Other available methods dependent on serum enzyme analysis or various imaging techniques generally show some distinct shortages such as unsatisfactory sensitivity and low specificity, making them unable to detect the AR before severe cell and tissue damage have occurred. Therefore, development of different means that are able to provide effective diagnosis of AR in a noninvasive way and at early stage remains a big challenge. In the present study, incorporation of the MRI T_2 contrast agent SPION turned the CD3-targeted gene vector into a MRI probe with high sensitivity. Consequently, the

polyplex carrying the DGKα gene, which was termed "theranostic nanosystem", was trackable *in vivo* in a noninvasive and dynamic manner. In our investigation, acute rejection was clearly detected 3 days after heart transplantation, upon injecting the CD3-targeted theranostic nanosystem *via* tail vein. When AR took place in rats, T cells accumulated in the allograft. Owing to the recognition of the CD3 antigen on T cells, the CD3-targeted theranostic nanosystem binds to T cells specifically, which resulted in the signal intensity change observable with MRI. The nontargeted nanocomplex could not specifically bind to T cells and thus could not act as an effective probe for T-cell accumulation. *In vivo* studies of fluorescent imaging and histologic studies verified the accuracy of the targeted theranostic nanosystem in probing T-cell accumulation in the transplanted heart that was observed on the noninvasive MRI.

***In Vivo* Toxicological and Organ Distribution.** The side effects and organ distribution of the polyplexes as a possible future therapeutic approach shall be determined after being delivered *in vivo* to animals. The serum biochemical tests including alanine transaminase (ALT) level and total bilirubin (TBIL) were detected to evaluate the liver function state. Further histological analysis was performed to determine the structure damage of livers after injection of the polyplexes. The serum ALT level is a sensitive biomarker for mild hepatocellular damage, and the increased TBIL level is indicative of severe damage of liver. As shown in Figure 7, only a mild, transient increase of ALT level occurred, while no obvious change in TBIL levels was present in TD and PBS groups. Histological analysis showed no obvious structural damage of the livers. These results suggested that the polyplexes can only cause a transient liver functional abnormality, however, without a substantial detrimental effect on the liver structure.

To determine the *in vivo* distribution of the polyplexes, we synthesized a manganese-doped SPION that was used in place of native SPION to produce the Mn-doped scAbCD3-PEG-g-PEI-SPION/pDNA-DGKα (scAbCD3-PEG-g-PEI-Mn-SPION/pDNA-DGKα) or PEG-g-PEI-SPION/pDNA-DGKα (PEG-g-PEI-Mn-SPION/pDNA-DGKα). Through detecting Mn content in organs of the heart transplanted rats after injection of scAbCD3-PEG-g-PEI-Mn-SPION/pDNA-DGKα or PEG-g-PEI-Mn-SPION/pDNA-DGKα at a Mn dose of 30 μg using atomic absorption spectrophotometry (AAS), the fraction of nanocarriers deposited in the organs could be indirectly measured. As shown in Figure S7 in Supporting Information, the percentage of Mn in the spleen and grafted heart to the total infused dosage was higher in the animals treated with scAbCD3-PEG-g-PEI-Mn-SPION/pDNA-DGKα than with PEG-g-PEI-Mn-SPION/pDNA-DGKα ($P < 0.05$), while no significant difference in Mn content was detected in livers or native hearts. This suggests that the presence of CD3 targeting in the polyplex may influence the *in vivo* organ distribution of nanocarriers. The CD3-targeted polyplex shows a tendency of accumulation in the organs that have a higher number of T cells such as the spleen or have abnormal T-cell infiltration such as the grafted heart showing strong acute immuno-rejection.

CONCLUSION

In summary, the immune response present in the allogeneic heart transplantation rat model was significantly suppressed upon gene therapy mediated by a CD3-targeted theranostic nanosystem, as confirmed by systematic histological and molecular studies. More importantly, this immune process was readily monitored by using the clinically available noninvasive MRI, on which the visualization of not only the allograft rejection events but also the immuno-suppressive effect of the gene therapy can be assessed simultaneously. For the gene therapy *via* the theranostic nanosystem, functionalization with the T-cell-targeted CD3 single-chain antibody played a key role in probing T-cell gathering and achieving optimized immunomodulation of T cells. Such a theranostic nanosystem has the great potential to provide coincident real-time monitoring and effective immuno-suppression of acute rejection after organ transplantation. Although the preliminary *in vivo* toxicological and organ distribution studies revealed no substantial liver damage and a preferred distribution in the grafted heart, more *in vivo* toxicological studies and comprehensive *in vivo* distribution tests using radioisotope incorporated nanocarriers to resolve the issues regarding pharmacokinetics, distribution, and elimination will be required before this theranostic nanosystem can be applied in humans. In the present AR model, the CD3-targeted theranostic nanosystem showed a dominant protective effect, which may be reasonably assumed to be the inhibition of cytotoxic T cells and pro-inflammatory subtypes of T-helper cells (TH1, TH17). Nevertheless, it is noteworthy that, as the CD3 antigen is a universal marker for T cells, the immuno-suppressive T-helper subsets (natural and inducible Treg) that play an important role in establishing and maintaining self-tolerance could be targeted, as well. In this sense, a polyplex with the capacity of identifying the T-cell subsets through targeting cytokine profiles or specific transcription factors could be more profitable, which will be further investigated in our future study.

MATERIALS AND METHODS

Materials. Fluorescent labeling agents 4′,6-diamidino-2-phenylindole (DAPI), POPO-3, Oregon Green 488, and Alexa Fluor 680 were purchased from Molecular Probes, Inc. (Eugene, OR, USA). Anti-rat CD3 antibody, PE-labeled CD3 antibody, and CD3 isotype control antibody were purchased from BD Bioscience

Pharmingen (San Jose, CA, USA), and mouse anti-rat IL-2 antibody and mouse anti-rat DGKα antibody were purchased from Santa Cruz Biotechnology, Inc. (Santa Cruz, CA, USA). HRP-labeled goat anti-mouse secondary antibody was purchased from Biomedical Technologies Inc. (Stoughton, MA, USA). Synthesis and characterization of the nonviral delivery agents (PEG-g-PEI, PEG-g-PEI-SPION and scAbCD3-PEG-g-PEI-SPION) were described in detail in our previous report.[16] The therapeutic pcDNA3.1-DGKα and null pcDNA3.1 plasmids were described in our previous report and used in the present study, as well.[16] The plasmid DNAs were amplified using *Escherichia coli* and purified according to the manufacturer's instructions of EndoFree Plasmid Giga Kits (QIAGEN, CA, USA). The purified pDNAs were kept in endotoxin-free TE buffer at a concentration of 2.4 mg/mL prior to use.

Inbred male Lewis rats (250−300 g) and Brown-Norway rats (250−300 g) from Vital River Laboratories (Beijing, China) were used as recipients and donors, respectively. The animals were maintained under SPF environment in the animal facility before and after the allogeneic abdominal heterotopic heart transplantation. All studies involving animals were approved by the Institutional Animal Care and Use Committee of Sun Yat-Sen University.

Primary mononuclear cells (MNCs) were isolated from the peripheral blood of Lewis rats using density gradient centrifugation on NycoPrep 1.077A (Axis-Shield, Oslo, Norway), and then cultured in RPMI 1640 medium (GIBCO, Invitrogen, USA) supplemented with 10% (v/v) fetal bovine serum (FBS) and kept at 37 °C in humidified atmosphere containing 5% CO_2. T cells were sorted by flow cytometry with CD3 antibody.[25−27]

***In Vitro* Cytotoxicity Assay.** Cytotoxicity of the polyplexes was evaluated *in vitro* using the CCK-8 assay with cell counting kit-8 (Dojindo, Kumamoto, Japan), according to the manufacturer's manual. All experiments were conducted in quadruplicate, and the following vectors were tested to assess the polyplex cytotoxicity: PEI/pDNA, PEG-g-PEI-SPION/pDNA, and scAbCD3-PEG-g-PEI-SPION/pDNA. For cytotoxicity test, the polyplexes used for the cytotoxicity test were formed at various N/P ratios, and rat T cells were seeded in 96-well plates at a density of 1×10^6 cells/well. RPMI 1640 cell culture medium (0.2 mL) was added to each well, and the pDNA mass in each well was set to 0.15 mg. After cell incubation for 48 h in the presence of polyplex, 10 mL of CCK-8 solution was added. The cells were further incubated for 8 h, and then the absorbance at 570 and 690 nm was recorded on a Tecan Infinite F200 Multimode plate reader.

Internalization of Polyplexes into Primary T Cells. To enable CLSM observation of the cells after incubation, the delivery agent scAbCD3-PEG-g-PEI-SPION was labeled with Oregon Green 488 and pDNA-DGKα was labeled with POPO-3 according to the manufacturer's protocols.[16] The T cells were seeded in 6-well plates at a density of 1×10^6 cells per well and cultured with the RPMI 1640 medium. pDNA-DGKα and the delivery agent scAbCD3-PEG-g-PEI-SPION were labeled with POPO-3 and Oregon Green 488, respectively, and then dissolved separately in aqueous solutions of 0.9% sodium chloride. The two solutions were mixed at N/P of 10 by vigorous pipetting, and then the mixture was kept at room temperature for 60 min to allow the formation of the polyplex of pDNA and delivery agent. Subsequently, the polyplex solution was added into the RPMI 1640 culture medium at a pDNA dose of 4 μg per well. After 1 h incubation, the cells were washed three times with PBS and fixed for 30 min in the presence of 4% paraformaldehyde solution. After the cells were washed again with PBS, the DNA-staining agent DAPI (1 mg/mL) was added and then the cells were further incubated for 30 min. The cells were collected, pipetted onto the glass slide, and allowed to dry in ambient conditions. A Zeiss LSM 510 META microscope (Carl Zeiss Inc., Göttingen, Germany) was used to observe cell fluorescence. For fluorescence excitation of Oregon Green 488, an Enterprise UV laser with an excitation wavelength of 488 nm was used, and for excitation of POPO-3, a helium−neon laser with an excitation wavelength of 534 nm was used. Excitation of DAPI was performed using an argon laser with an excitation wavelength of 358 nm.

Cell Transfection. Cell transfection experiment was carried out using the polyplex (scAbCD3-PEG-g-PEI-SPION/pDNA-EGFP) formed at the N/P ratio of 10. T cells obtained from the peripheral blood of Lewis rats were resuspended in RPMI 1640 medium and added into 6-well plates at a density of 1×10^6 cells per well. Then, the polyplex solution was added to incubate the cells for 8 h. After the medium inside the wells was discarded, the cells were washed with fresh RPMI 1640 and further incubated for 40 h before measuring gene transfection level. To examine the expression level of EGFP in T cells, the cells were collected and observed on a Carl Zeiss Aviox-1 inverted fluorescence microscope. Quantitative analysis of the cell uptake of the polyplex was conducted on a FACScan flow cytometer. We use the percentage of EGFP-positive cells in total cells as the transfection efficiency. Western blotting with anti-DGKα antibody was conducted to evaluate the expression level of therapeutic gene in primary T cells at day 3 after DGKα gene transfection as published previously.[16] To evaluate the gene level of DGKα, reverse transcription PCR was performed, as well. The detection of the bands was performed using a VersaDoc model 5000 imaging system quantifying their intensity with the Quantity One computer software (Bio-Rad). The densitometry of the bands in relation to PBS incubation was normalized to the corresponding actin band.

Rat Allogeneic Heart Transplantation Model. Heterotopic heart transplantation in rats (BN to LEW) was performed according to the method of Ono and Lindsey with minor modifications.[28−31] In brief, the donor heart was transplanted into the recipient's abdominal cavity by anastomosing the donor arteriae aorta and the pulmonary artery to the recipient's abdominal aorta and inferior vena cava, respectively. The transplanted heart was located in the right infrarenal abdomen and thus contractions can be palpated through the abdominal wall. Overall, 60 transplantations were performed for *in vivo* imaging and therapeutic studies, and the animals were divided into four groups for the AR study. All experimental procedures involving animals were in accordance with the Guide for the Care and Use of Laboratory Animals (NIH publication nos. 80-23, revised 1996) and were performed according to the institutional ethical guidelines for animal experiment.

***In Vivo* Studies.** The Lewis rats bearing heterotopic cardiac allograft were equally divided into five groups (n = 12) and treated with scAbCD3-PEG-g-PEI-SPION/pDNA-DGKα (TD group), scAbCD3-PEG-g-PEI-SPION/pDNA (TN group), PEG-g-PEI-SPION/pDNA-DGKα (ND group), PEG-g-PEI-SPION/pDNA (NN group), and PBS injection (PBS group) after the allogeneic heart transplantation at one injection per day for 10 days. Polyplex dissolved in 500 μL of PBS was injected *via* the tail vein at a pDNA dose of 100 μg per injection, and the same volume of PBS alone was injected in the PBS control group. As heart beating of transplanted heart can be assessed *in vivo* and had been used as the main indicator to judge the development of AR and graft survival, the palpation of the abdomen to access beating of the allograft was performed by a blinded investigator on all animals daily. The development of AR was evaluated by heart beating score (HBS) according to a semiquantitative scoring from 0 (no palpable contractions) to 4 (strong contractions), where score 0 was 0 beats per minute (bpm); score 1, 1−40 bpm; score 2, 41−80 bpm; score 3, 81−120 bpm; score 4, >120 bpm. HBS > 0 was considered to indicate the graft survival, while grafts were considered as rejected when the HBS = 0 as measured by palpation. Graft survival was recorded until the end point of the study, and graft survival time was expressed as the mean graft survival time.[32]

***In Vivo* MRI.** On the first day after transplantation, *in vivo* MRI was performed at 0 and 2 h after the rats were treated with a polyplex or PBS. After anesthesia, animals were placed in the prone position. MRI was performed on a clinical 1.5 T MRI scanner (Intera; Philips Medical Systems, Best, The Netherlands) at room temperature using a 5 cm linearly polarized birdcage radio frequency rat coil (Chenguang Medical Technologies Co., Shanghai, China). MRI was repeated on the third and tenth days at 2 h after the injection.

Axial images of the transplanted heart, native heart, and liver and spleen of each animal were obtained by using balanced turbo field echo (bTFE) pulse sequence. The acquisition parameters were TR/TE = 200/6 ms; FOV = 70 mm; flip angle = 90°; matrix = 256 × 256; section thickness = 2.0 mm; number of signal acquisition (NSA) = 1. T_2 relaxation data of the transplanted heart were also

acquired using a single-section multispin−echo sequences with the following parameters: TR = 2000 ms, TE = 20 ms, stepped echo time = 20−160 ms for eight steps; echo spacing = 20 ms; FOV = 70 mm; matrix = 256 × 256; section thickness = 2.0 mm. T_2 maps were calculated from the respective T_2 relaxation data by using the available software tools provided by the manufacturer, which are based on the least-squares algorithms. The change of signal intensity on the bTFE images was visually observed and was further confirmed with T_2 maps.

***In Vivo* NIRF Imaging.** The polyplexes were dissolved in 0.1 M sodium bicarbonate buffer at 0.5 mg/mL (component A), then the amine-reactive compound Alexa Fluor 680 was dissolved in DMSO at 10 mg/mL (component B). While stirring the agent solution (component A), we slowly added the reactive dye solution (component B) in 1:10 dilutions. The reaction was conducted for 1 h at room temperature under continuous stirring. The unreacted labeling reagent was eliminated from the solution by ultrafiltration in an Amicon cell (regenerated cellulose membrane, MWCO = 5 kDa). The dye-conjugated polyplex solutions thus prepared were washed several times with pH 7.4 PBS until no absorption at 680 nm was detectable in the filtrate. Optical imaging was performed using a whole-body animal imaging system (Imaging Station IS2000MM, Eastman Kodak, Rochester, NY, USA) equipped with an appropriate band-pass filter at 625 nm and a long-pass filter at 710 nm 2 h after the rats were treated as previously mentioned. Image reconstruction was performed using the Kodak Molecular Imaging Software. The delivery agents of TN, TD, NN, and ND groups labeled with Alexa Fluor 680 were injected intravenously to assess the organ localization of nanoparticles.[33]

Histological and Immunohistochemical Analyses. To evaluate the development of AR after transplantation, full-thickness midventricular sections of the implanted hearts were collected on the tenth days post-transplantation and then underwent Prussian blue staining and counterstaining with hematoxylin and eosin (H&E staining). Prussian blue staining can be used to detect the incorporated iron complex in the cells after incubation.[34] Cells with SPION internalization will be stained in blue, which is indicative of cellular uptake of the polyplex. AR was assessed with at least three slides for each specimen and was scored according to the grading system of the International Society for Heart and Lung Transplantation (ISHLT), which is defined as follows: score 0, no rejection; IA, focal infiltrate of large lymphocytes without myocyte damage; IB, diffuse but sparse infiltrate without myocyte damage; II, one focus only with aggressive infiltrate and/or focal myocyte damage; IIIA, multifocal aggressive infiltrates and/or myocyte damage; IIIB, diffuse inflammatory process with nerosis; IV, diffuse aggressive polymorphous infiltrate ± edema, ± hemorrhage, ± vasculitis with nerosis.[35] The final scores used for AR were based on an average of three specimens from each heart. The AR was assessed in a blinded manner. For the detection of CD3-positive T cells, contiguous sections of the formalin-fixed and paraffin-embedded samples were observed in a blinded manner.

For the immuno-histochemical analysis, the samples on slides were deparaffinized with xylol, rehydrated through a series of ethanol (100, 95, 80, then 70%), and then rinsed well under running distilled water. After heat-inactivated epitope retrieval with preheated retrieval buffer (0.1 mmol EDTA, pH 8.0), the slides were incubated with 0.3% H_2O_2 for 10 min at room temperature to eliminate endogenous peroxidase activity, then incubated in 1:100 dilutions in PBST buffer of mouse anti-rat IL-2 antibody or mouse anti-rat DGKα antibody for 40 min. After washing with PBS, the slides were further incubated for 20 min with HRP-labeled goat anti-mouse secondary antibody. Finally, the immuno-reactivity on the tissue sections was visualized using streptavidin peroxidase for color development with 3-amino-9-ethylcarbazole (AEC) as substrate.

***In Vivo* Toxicological and Organ Distribution Studies.** To determine the side effects of the polyplexes, the heart transplanted rats were equally divided into three groups (n = 12 each) to receive single injection of scAbCD3-PEG-g-PEI-SPION/pDNA-DGKα (TD group), PEG-g-PEI-SPION/pDNA-DGKα (ND group), and PBS on the third day after the allogeneic heart transplantation. The polyplexes were dissolved in 500 μL of PBS and were injected *via* the tail vein at a pDNA dose of 100 μg per injection, and the same volume of PBS alone was injected in the PBS control group. To determine the state of the liver, serum biochemical tests including alanine transaminase (ALT) and total bilirubin (TBIL) were performed using serum ALT assay kits and TBIL assay kits (Sigma, St. Louis, MO, USA) over 64 h after the injection. To further determine the structural liver injury, sections of the liver were collected and processed for H&E staining when the biochemical tests of liver function were completed.

To determine the *in vivo* distribution of the polyplexes, manganese-doped SPION (Mn-SPION) was first synthesized following a previously published procedure.[36] Then, the obtained Mn-doped SPION was used in place of the native SPION to produce the polyplexes scAbCD3-PEG-g-PEI-Mn-SPION/pDNA-DGKα and PEG-g-PEI-Mn-SPION/pDNA-DGKα, in the same manner as described.[16] Twenty four heart transplanted rats were divided into two groups (n = 12 each) to receive single injection of scAbCD3-PEG-g-PEI-Mn-SPION/pDNA-DGKα or PEG-g-PEI-Mn-SPION/pDNA-DGKα *via* the tail vein at a Mn dose of 30 μg. Three hours after the injection, the entire liver, spleen, grafted heart, and native heart of animals were harvested, freeze-dried in liquid nitrogen, and grounded into powder. The fine powdery samples were weighed and then treated with a 10 mL mixture of hydrochloric acid and nitric acid (1:1 v/v) for 5 days to allow for polymer degradation and complete dissolution of Mn-SPION. Mn concentration was then measured by atomic absorption spectrophotometry using a polarized Zeeman atomic absorption spectrophotometer (model Z-2000, Hitachi, Japan) at the specific Mn absorption wavelength (279.5 nm) based on a pre-established calibration curve. The Mn content deposited was calculated as the percentage of Mn in individual organ to the total dosage of infused Mn.

Statistical Analysis. Data were expressed as mean ± SD. Statistical analysis of data was performed with Student's t tests using the one-way analysis of variance. $P < 0.05$ was considered to indicate statistical significance. All statistical tests were performed with SPSS software (version 13.0, SPSS Inc.).

Conflict of Interest: The authors declare no competing financial interest. ‖These authors contributed equally to this work.

Acknowledgment. This work was supported by the Natural Science Foundation of China 50830107 and 81071208, the 863 Programs of the Ministry of Science and Technology of China 2009AA03Z310, Specialized Research Fund for the Doctoral Program of Higher Education (SRFDP) 20110171120091.

Supporting Information Available: The particle size of the polyplex in the rat serum and PBS; cellular uptake experiment with a CD3 isotype control antibody-conjugated polyplex; *in vivo* MR and NIRF imaging of heart transplantation rat model receiving different treatments; *in vivo* MR and NIRF imaging of the spleens in heart transplantation rat model; IL-2 expression determined by ELISA assay in the periphery blood of heart transplanted rats; primary T cell proliferation determined by [^{3}H] thymidine assay; *in vivo* organ distribution of the polyplexes. This material is available free of charge *via* the Internet at http://pubs.acs.org.

REFERENCES AND NOTES

1. Levitsky, J. Operational Tolerance: Past Lessons and Future Prospects. *Liver Transplant.* **2011**, *17*, 222–232.
2. Patel, J. K.; Kittleson, M.; Kobashigawa, J. A. Cardiac Allograft Rejection. *Surgeon* **2011**, *9*, 160–167.
3. Bluestone, J. A. Mechanisms of Tolerance. *Immunol. Rev.* **2011**, *241*, 5–19.
4. Mirabet, S.; Gelpí, C.; Roldán, C.; Brossa, V.; Mendoza, C. A.; Lopez, L.; Molto, E.; Alvaro, Y.; Martinez, V.; Padró, J. M.; *et al.* Assessment of Immunological Markers as Mediators of Graft Vasculopathy Development in Heart Transplantation. *Transplant Proc.* **2011**, *43*, 2253–2256.
5. Halawa, A. The Early Diagnosis of Acute Renal Graft Dysfunction: A Challenge We Face. The Role of Novel Biomarkers. *Ann. Transplant.* **2011**, *16*, 90–98.
6. Devarajan, P. Biomarkers for the Early Detection of Acute Kidney Injury. *Curr. Opin. Pediatr.* **2011**, *23*, 194–200.

7. Szederkényi, E.; Iványi, B.; Morvay, Z.; Szenohradszki, P.; Borda, B.; Marofka, F.; Kemény, E.; Lázár, G. Treatment of Subclinical Injuries Detected by Protocol Biopsy Improves the Long-Term Kidney Allograft Function: A Single Center Prospective Randomized Clinical Trial. *Transplant Proc.* **2011**, *43*, 1239–1243.
8. Kozlowski, T.; Rubinas, T.; Nickeleit, V.; Woosley, J.; Schmitz, J.; Collins, D.; Hayashi, P.; Passannante, A.; Andreoni, K. Liver Allograft Antibody-Mediated Rejection with Demonstration of Sinusoidal C4d Staining and Circulating Donor-Specific Antibodies. *Liver Transplant.* **2011**, *17*, 357–368.
9. Tilney, N. L.; Strom, T. B.; Kupiec-Weglinski, J. W. Humoral and Cellular Mechanisms in Acute Allograft Injury. *J. Pediatr.* **1987**, *111*, 1000–1003.
10. Murphy, S. P.; Porrett, P. M.; Turka, L. A. Innate Immunity in Transplant Tolerance and Rejection. *Immunol. Rev.* **2011**, *241*, 39–48.
11. Fahmy, T. M.; Fong, P. M.; Park, J.; Constable, T.; Saltzman, W. M. Nanosystems for Simultaneous Imaging and Drug Delivery to T Cells. *AAPS J.* **2007**, *9*, E171–E180.
12. Liu, J.; Farmer, J. D., Jr.; Lane, W. S.; Friedman, J.; Weissman, I.; Schreiber, S. L. Calcineurin Is a Common Target of Cyclophilin-Cyclosporin A and FKBP-FK506 Complexes. *Cell.* **1991**, *66*, 807–815.
13. Nasongkla, N.; Shuai, X.; Ai, H.; Weinberg, B. D.; Pink, J.; Boothman, D. A.; Gao, J. cRGD-Functionalized Polymer Micelles for Targeted Doxorubicin Delivery. *Angew. Chem., Int. Ed.* **2004**, *43*, 6323–6327.
14. Lee, J.; Yun, K.-S.; Choi, C. S.; Shin, S.-H.; Ban, H.-S.; Rhim, T.; Lee, S. K.; Lee, K. Y. T Cell-Specific siRNA Delivery Using Antibody-Conjugated Chitosan Nanoparticles. *Bioconjugate Chem.* **2012**, *23*, 1174–1180.
15. Nasongkla, N.; Bey, E.; Ren, J.; Ai, H.; Khemtong, C.; Guthi, J. S.; Chin, S. F.; Sherry, A. D.; Boothman, D. A.; Gao, J. Multifunctional Polymeric Micelles as Cancer-Targeted, MRI-Ultrasensitive Drug Delivery Systems. *Nano Lett.* **2006**, *6*, 2427–2430.
16. Chen, G.; Chen, W.; Wu, Z.; Yuan, R.; Li, H.; Gao, J.; Shuai, X. MRI-visible Polymeric Vector Bearing CD3 Single Chain Antibody for Gene Delivery to T Cells for Immunosuppression. *Biomaterials* **2009**, *30*, 1962–1970.
17. Olenchock, B. A.; Guo, R.; Carpenter, J. H.; Jordan, M.; Topham, M. K.; Koretzky, G. A.; Zhong, X. P. Disruption of Diacylglycerol Metabolism Impairs the Induction of T Cell Anergy. *Nat. Immunol.* **2006**, *7*, 1174–1181.
18. Sanjuán, M. A.; Pradet-Balade, B.; Jones, D. R.; Martínez-A, C.; Stone, J. C.; Garcia-Sanz, J. A.; Mérida, I. T Cell Activation *In Vivo* Targets Diacylglycerol Kinase Alpha to the Membrane: A Novel Mechanism for Ras Attenuation. *J. Immunol.* **2003**, *170*, 2877–2883.
19. Cormack, B. P.; Valdivia, R. H.; Falkow, S. FACS-Optimized Mutants of the Green Fluorescent Protein (GFP). *Gene* **1996**, *173*, 33–38.
20. Saleem, S. N. Feasibility of MRI of the Fetal Heart with Balanced Steady-State Free Precession Sequence Along Fetal Body and Cardiac Planes. *AJR, Am. J. Roentgenol.* **2008**, *191*, 1208–1215.
21. Burchill, M. A.; Yang, J.; Vang, K. B.; Farrar, M. A. Interleukin-2 Receptor Signaling in Regulatory T Cell Development and Homeostasis. *Immunol. Lett.* **2007**, *114*, 1–8.
22. Cheng, G.; Yu, A.; Malek, T. R. T-Cell Tolerance and the Multi-Functional Role of IL-2R Signaling in T-Regulatory Cells. *Immunol. Rev.* **2011**, *241*, 63–76.
23. Bour-Jordan, H.; Esensten, J. H.; Martinez-Llordella, M.; Penaranda, C.; Stumpf, M.; Bluestone, J. A. Intrinsic and Extrinsic Control of Peripheral T-Cell Tolerance by Costimulatory Molecules of the CD28/B7 Family. *Immunol. Rev.* **2011**, *241*, 180–205.
24. Flögel, U.; Su, S.; Kreideweiss, I.; Ding, Z.; Galbarz, L.; Fu, J.; Jacoby, C.; Witzke, O.; Schrader, J. Noninvasive Detection of Graft Rejection by *In Vivo* (19) F MRI in the Early Stage. *Am. J. Transplant.* **2011**, *11*, 235–244.
25. Park, J. H.; Lee, S.; Kim, J. H.; Park, K.; Kim, K.; Kwon, I. C. Polymeric Nanomedicine for Cancer Therapy. *Prog. Polym. Sci.* **2008**, *33*, 113–137.
26. Miyata, K.; Christie, R. J.; Kataoka, K. Polymeric Micelles for Nano-Scale Drug Delivery. *React. Funct. Polym.* **2011**, *71*, 227–234.
27. Davey, H. M.; Kell, D. B. Flow Cytometry and Cell Sorting of Heterogeneous Microbial Populations: The Importance of Single-Cell Analyses. *Microbiol. Rev.* **1996**, *60*, 641–696.
28. Jung, T.; Schauer, U.; Heusser, C.; Neumann, C.; Rieger, C. Detection of Intracellular Cytokines by Flow Cytometry. *J. Immunol. Methods* **1993**, *159*, 197–207.
29. Shan, J.; Huang, Y.; Feng, L.; Luo, L.; Li, C.; Ke, N.; Zhang, C.; Li, Y. A Modified Technique for Heterotopic Heart Transplantation in Rats. *J. Surg. Res.* **2010**, *164*, 155–161.
30. Ricci, D.; Mennander, A. A.; Miyagi, N.; Rao, V. P.; Tazelaar, H. D.; Classic, K.; Byrne, G. W.; Russell, S. J.; McGregor, C. G. Prolonged Cardiac Allograft Survival Using Iodine 131 after Human Sodium Iodide Symporter Gene Transfer in a Rat Model. *Transplant Proc.* **2010**, *42*, 1888–1894.
31. Doenst, T.; Schlensak, C.; Kobba, J. L.; Beyersdorf, F. A Technique of Heterotopic, Infrarenal Heart Transplantation with Double Anastomosis in Mice. *J. Heart Lung Transplant.* **2001**, *20*, 762–765.
32. Deuse, T.; Velotta, J. B.; Hoyt, G.; Govaert, J. A.; Taylor, V.; Masuda, E.; Herlaar, E.; Park, G.; Carroll, D.; Pelletier, M. P; *et al.* Novel Immunosuppression: R348, a JAK3- and Syk-Inhibitor Attenuates Acute Cardiac Allograft Rejection. *Transplantation* **2008**, *85*, 885–892.
33. Ogawa, M.; Regino, C. A.; Choyke, P. L.; Kobayashi, H. *In Vivo* Target-Specific Activatable Near Infrared Optical Labeling of Humanized Monoclonal Antibodies. *Mol. Cancer Ther.* **2009**, *8*, 232–239.
34. Genove, G.; DeMarco, U.; Xu, H.; Goins, W. F.; Ahrens, E. T. A New Transgene Reporter for *In Vivo* Magnetic Resonance Imaging. *Nat. Med.* **2005**, *11*, 450–454.
35. Billingham, M. E.; Cary, N. R.; Hammond, M. E.; Kemnitz, J.; Marboe, C.; McCallister, H. A.; Snovar, D. C.; Winters, G. L.; Zerbe, A. A Working Formulation for the Standardization of Nomenclature in the Diagnosis of Heart and Lung Rejection: Heart Rejection Study Group. The International Society for Heart Transplantation. *J. Heart Transplant.* **1990**, *9*, 587–593.
36. Sun, S.; Zeng, H.; Robinson, D. B.; Raoux, S.; Rice, P. M.; Wang, S. X.; Li, G. Monodisperse MFe_2O_4 (M = Fe, Co, Mn) Nanoparticles. *J. Am. Chem. Soc.* **2004**, *126*, 273–279.